



OPEN ACCESS

EDITED BY

Leiliang Zhang,
Shandong First Medical University and
Shandong Academy of Medical
Sciences, China

REVIEWED BY

Junjie Zhang,
Wuhan University, China
Mengmeng Zhao,
Foshan University, China

*CORRESPONDENCE

Haixue Zheng
✉ zhenghaixue@caas.cn

[†]These authors have contributed equally to
this work

RECEIVED 18 April 2024

ACCEPTED 27 May 2024

PUBLISHED 17 June 2024

CITATION

Zhang D, Hao Y, Yang X, Shi X, Zhao D,
Chen L, Liu H, Zhu Z and Zheng H (2024) ASFV
infection induces macrophage necroptosis
and releases proinflammatory cytokine by
ZBP1-RIPK3-MLKL necrosome activation.
Front. Microbiol. 15:1419615.
doi: 10.3389/fmicb.2024.1419615

COPYRIGHT

© 2024 Zhang, Hao, Yang, Shi, Zhao, Chen,
Liu, Zhu and Zheng. This is an open-access
article distributed under the terms of the
[Creative Commons Attribution License \(CC
BY\)](https://creativecommons.org/licenses/by/4.0/). The use, distribution or reproduction in
other forums is permitted, provided the
original author(s) and the copyright owner(s)
are credited and that the original publication
in this journal is cited, in accordance with
accepted academic practice. No use,
distribution or reproduction is permitted
which does not comply with these terms.

ASFV infection induces macrophage necroptosis and releases proinflammatory cytokine by ZBP1-RIPK3-MLKL necrosome activation

Dajun Zhang[†], Yu Hao[†], Xing Yang, Xijuan Shi, Dengshuai Zhao,
Lingling Chen, Huanan Liu, Zixiang Zhu and Haixue Zheng*

State Key Laboratory for Animal Disease Control and Prevention, College of Veterinary Medicine,
Lanzhou University, Lanzhou Veterinary Research Institute, Chinese Academy of Agricultural Sciences,
Lanzhou, China

African swine fever (ASF) is an infectious disease characterized by hemorrhagic fever, which is highly pathogenic and causes severe mortality in domestic pigs. It is caused by the African swine fever virus (ASFV). ASFV is a large DNA virus and primarily infects porcine monocyte macrophages. The interaction between ASFV and host macrophages is the major reason for gross pathological lesions caused by ASFV. Necroptosis is an inflammatory programmed cell death and plays an important immune role during virus infection. However, whether and how ASFV induces macrophage necroptosis and the effect of necroptosis signaling on host immunity and ASFV infection remains unknown. This study uncovered that ASFV infection activates the necroptosis signaling *in vivo* and macrophage necroptosis *in vitro*. Further evidence showed that ASFV infection upregulates the expression of ZBP1 and RIPK3 to consist of the ZBP1-RIPK3-MLKL necrosome and further activates macrophage necroptosis. Subsequently, multiple Z-DNA sequences were predicted to be present in the ASFV genome. The Z-DNA signals were further confirmed to be present and colocalized with ZBP1 in the cytoplasm and nucleus of ASFV-infected cells. Moreover, ZBP1-mediated macrophage necroptosis provoked the extracellular release of proinflammatory cytokines, including TNF- α and IL-1 β induced by ASFV infection. Finally, we demonstrated that ZBP1-mediated necroptosis signaling inhibits ASFV replication in host macrophages. Our findings uncovered a novel mechanism by which ASFV induces macrophage necroptosis by facilitating Z-DNA accumulation and ZBP1 necrosome assembly, providing significant insights into the pathogenesis of ASFV infection.

KEYWORDS

ASFV, host macrophages, necroptosis signaling, ZBP1, Z-DNA, proinflammatory cytokines

1 Introduction

African swine fever (ASF), caused by the African swine fever virus (ASFV), is an extremely contagious and highly fatal disease in domestic pigs and wild boars. The spread of ASF worldwide has severely impacted the pig industry over the past century (Gallardo et al., 2015). In 2018, ASF broke out in China and spread rapidly throughout the country, causing great economic loss and posing a serious threat to Chinese pork safety and supply

(Sanchez-Cordon et al., 2018; Zhou et al., 2018). Unfortunately, since there are currently no effective vaccines or drugs for ASFV, ASF prevention relies solely on the rapid culling of susceptible animals and strict epidemic control measures (Urbano and Ferreira, 2022).

ASFV, the only member of the *Asfarviridae* family, is a large, enveloped, double-stranded (ds) DNA virus (Alonso et al., 2018). The dsDNA genome length of ASFV ranges from 170 to 194 kb encoding more than 150 proteins indispensable to viral replication, transcription, and host immune evasion (Wang Y. et al., 2021). ASFV mainly infects porcine monocyte macrophages, and the interaction between ASFV and porcine macrophages is the main cause of ASFV pathogenesis (Carrasco et al., 1996; Salguero et al., 2002; Zheng et al., 2022). However, the interaction between ASFV and porcine macrophages remains not fully articulated, even with much effort.

Programmed cell death (PCD) may act as an immune mechanism to restrict pathogen infection and enhance viral release and pathogenesis. ASFV infection causes the macrophages' apoptosis dependent on caspases 3, 7, 9, and 12 (Galindo et al., 2012; Li T. et al., 2021). Tumor necrosis factor α (TNF- α)-dependent extrinsic apoptosis was induced in porcine alveolar macrophages (PAMs) infected with ASFV (Zheng et al., 2022). ASFV has also evolved multiple viral proteins, maintaining its fast replication by interfering with host apoptosis machinery. For example, A179L, a Bcl-homolog encoded ASFV, can inhibit mitochondrial apoptosis by interacting with the BH3 domain of pro-apoptotic Bcl-2 family proteins (Galindo et al., 2008). Further, ASFV A224L, an IAP-like protein, suppresses the proteolytic cleavage of caspase 3 (Nogal et al., 2001). In addition to apoptosis, pyroptosis, an inflammatory PCD characterized by the activation of the inflammasome, maturation of inflammatory cytokines, and plasma membrane damage, is also hijacked by ASFV (Yu et al., 2021). ASFV-encoded pS273R relieves the pyroptotic cell death by inactivating execution protein gasdermin D (GSDMD) (Zhao et al., 2022), and the interaction between ASFV pH240R and host NLRP3 inhibits macrophage pyroptosis by limiting NLRP3 oligomerization and IL-1 β production (Zhou et al., 2022).

Necroptosis, a caspase-independent inflammatory PCD similar to pyroptosis, induces intense inflammation by promoting the damage of the plasma membrane and releasing the inflammatory cytokines and damage-associated molecular patterns (DAMPs) into the cytoplasm (Kaczmarek et al., 2013). Initiation of necroptosis signaling requires the recruitment of receptor-interacting protein (RIP) homotypic interaction motif (RHIM)-containing RIP kinase 3 (RIPK3) to one of the other three RHIM-containing proteins, including receptor-interacting protein kinase 1 (RIPK1), TIR-domain-containing adapter-inducing interferon (TRIF), and Z-conformation nucleic acid (Z-NA) binding protein 1 (ZBP1) (Verdonck et al., 2022). After recruiting to other RHIM-containing proteins, RIPK3 phosphorylates interact with mixed lineage kinase domain-like protein (MLKL) to consist of a necrosome. Phosphorylated MLKL in necrosome polymerizes on the cytoplasmic membrane, forming membrane pores and driving plasma membrane leakage (Grootjans et al., 2017; Murphy, 2020). TNF- α induced RIPK1-RIPK3-MLKL necrosome, toll-like receptor (TLR) 3/4 mediated TRIF-RIPK3-MLKL necrosome, and

ZBP1-RIPK3-MLKL necrosome play a significant role in infectious diseases, such as herpesvirus (HSV), vaccinia virus (VACV), influenza A virus (IAV), and enteropathogenic *Escherichia coli* infection (Xia et al., 2020).

Porcine TNF- α is abundantly secreted in porcine serum and cell culture supernatants after ASFV infection (Carrasco et al., 2002; Salguero et al., 2002; Zheng et al., 2022). ASFV-encoded A179L also enhances RIPK1-dependent necroptosis induced by TNF- α in L929 cells (Shi et al., 2021). Moreover, TLR3/4 is activated to promote IL-1 β expression in ASFV-infected PAMs (Li J. et al., 2021). These past discoveries suggest ASFV-induced necroptosis signaling is possible via TNF- α -RIPK1 or TLR3/4-TRIF pathways. However, whether and how ASFV triggers the necroptosis signaling and what effect ASFV-induced necroptosis has on host immunity and ASFV infection remains unknown. Therefore, further research on the interaction between ASFV and macrophage necroptosis is necessary.

This study found that ASFV efficiently activates the necroptosis signaling in the porcine spleen, lung, liver, and kidney. We also confirmed that ASFV induces porcine macrophage necroptosis *in vitro*. Next, we demonstrated that ASFV-induced macrophage necroptosis was independent of TNF- α -RIPK1 or TLR-TRIF pathways but depended on upregulated ZBP1 in porcine macrophages. Furthermore, we uncovered that ASFV infection induces the formation of Z-conformation DNA (Z-DNA) to activate ZBP1-mediated necroptosis, causing the extracellular release of proinflammatory cytokines in porcine macrophages. ZBP1-mediated necroptosis signaling restricts ASFV replication in porcine macrophages. Our findings revealed an interaction mechanism between ASFV and porcine macrophage necroptosis that further elucidates the pathogenesis of ASFV.

2 Materials and methods

2.1 Animal experiments and ethics statement

Four landrace pigs aged 2 months and weighing \sim 25 Kg were obtained from a licensed livestock farm, with each pig being antigenically or serologically negative for ASFV, porcine reproductive and respiratory syndrome virus, pseudorabies virus, or porcine epidemic diarrhea virus, and classic swine fever virus. In this experiment, two random pigs were injected with ASFV/CN/GS/2018 (1.0 HAD50) as the ASFV infection group. The other two pigs were injected with phosphate-buffered saline as a mock infection group. Blood samples were collected from all pigs before 0 dpi, after injection, and at different time points after injection. Tissue samples were collected from two pigs infected with ASFV on day 9 and day 10 post-injection, respectively. Additionally, tissue samples were collected from two control pigs post-injection after euthanasia.

All animal experiments (including the euthanasia procedure) were performed in strict accordance with the Animal Ethics Procedures and Guidelines of the People's Republic of China and Accreditation of Laboratory Animal Care International and the Institutional Animal Care and Use Committee guidelines

(License No. SYXK [GAN] 2014–003). All experiments involving live ASFV were performed in the biosafety level 3 facilities of Lanzhou Veterinary Research Institute, Chinese Academy of Agricultural Sciences.

2.2 Cell culture and virus

Porcine alveolar macrophages (PAMs) were prepared using bronchoalveolar lavage as described previously and cultured in Roswell Park Memorial Institute (RPIM) 1640 medium (Gibco, USA) containing 10% porcine serum (Gibco, USA). Porcine bone marrow cells were harvested from the hip bone and femur of 8-week-old pigs. Harvested cells were cultured in RPIM 1640 medium containing 20% porcine serum and 10 ng/ml recombinant porcine granulocyte-macrophage colony-stimulating factor (GM-CSF, R&D Systems, UK) to differentiate mature bone marrow-derived macrophage (BMDMs) after 7 days. BMDMs were cultured in RPIM 1640 medium containing 20% porcine serum. Microbiological associates-104 (MA-104) cells were purchased from the China Center for Type Culture Collection (Wuhan, China) and cultured in Dulbecco's modified Eagle medium (Gibco, USA) with 10% fetal bovine serum (FBS, VivaCell, New Zealand). All cells were cultured in a humidified atmosphere containing 5% CO₂ at 37°C.

The CN/GS/2018 ASFV, a genotype II strain, was isolated and preserved by the Lanzhou Veterinary Research Institute, Chinese Academy of Agricultural Sciences. Viral titration of the strain was mensurated using the hemadsorption (HAD) assay and presented in HAD50 per milliliter.

2.3 Antibodies and reagents

Anti-B646L (ASFV P72 structure protein) mouse polyclonal antibody was prepared and provided by LVRI, CAAS. Anti-CP204L (ASFV P30 structure protein) mouse and rabbit monoclonal antibodies were presented by the College of Veterinary Medicine, Nanjing Agricultural University (Nanjing, China). Rabbit anti-Z-NA antibody (Z22) was purchased from Absolute Biotech Company (Oxford, UK). The following rabbit monoclonal antibodies were used: anti-Lamin A/C (4777S), anti-RIPK3 (13526S), anti-p-RIPK3 (91702S), anti-p-MLKL (37333S), anti-Myc-Tag (2272S), Alexa Fluor 488 anti-rabbit IgG (4416S), and Alexa Fluor 594 anti-mouse IgG (8890S) were purchased from Cell Signaling Technology (Massachusetts, USA); Anti-MLKL rabbit monoclonal antibody (ET1601-25) was purchased from HuaAn McAb Biotechnology Co, Ltd (<http://www.huabio.cn/>). Anti-β-actin mouse monoclonal antibody (66009-1-Ig), Horseradish peroxidase (HRP)-conjugated goat anti-mouse IgG (H+L; SA00001-1), HRP -conjugated goat anti-rabbit IgG (H+L; SA00001-2) were purchased from Proteintech Group Co., Ltd. (Chicago, IL, USA). Protein G Sepharose (17061801) was purchased from GE Healthcare Bio-sciences AB (Pittsburgh, PA, USA). HRP-conjugated goat anti-mouse IgG (SE131) was purchased from Beijing Solarbio Science and Technology Co., Ltd (Beijing, China).

Recombinant human IFN-β (300-02BC) was purchased from Peprotech (US). LPS (L8880) was purchased from Solarbio Life Science (Beijing, China). Recombinant porcine GM-CSF protein (711-PG-010) was purchased from R&D System (Minnesota, USA). SM-164 (HY-15989), Z-VAD-FMK (HY-16658B), Necrostatin-1 (HY-15760), GSK'872 (HY-101872), GW806742X (HY-112292), and Pepinh-TRIF (HY-P2565) were purchased from MedChemExpress (New Jersey, USA). Polyplus jetPRIME (PT-114-15) transfection reagent was purchased from Polyplus-Transfection SA (Strasbourg, France). Lipofectamin RNAiMAX transfection reagent was purchased from Thermo Fisher Scientific (California, USA).

2.4 Tissue protein extraction

One hundred milligram tissues were added to 800 μl of strong RIPA lysis buffer supplemented with protease and phosphatase inhibitor in 1.5 ml tubes. Sterile steel balls were added to each tube, and the tissue was fully ground using a TIANGEN H24 grinding homogenizer (Beijing, China); tissue proteins were then separated by centrifuging the tissue lysates (12,000 rpm, 10 min). Protein concentration was detected by a BCA kit (Thermo Fisher Scientific, 23227) and quantified to 5 μg/μl. The western blot assay was then carried out.

2.5 Plasmids construction and transfection

Plasmids encoding porcine ZBP1 (Gene ID: 100144524) and ZBP1ΔZα2 (deleting its Zα2 domain) were constructed by cloning the synthesized sequence into pcDNA3.1 with Myc tag fused to the 3' end. MA-104 cells were cultured in 12-well plates and transfected with 3 μg plasmids per well using Polyplus jetPRIME transfection reagent. After 8 h, cells were replaced with fresh DMEM culture medium. At 24 h post-transfection, cells were further treated or infected with ASFV.

2.6 siRNA interference

The siRNA duplexes targeting porcine ZBP1 were chemically synthesized by Gene-Pharma. ZBP1-specific siRNA duplexes were transfected into PAMs or BMDMs with RNAiMAX transfection reagents according to the manufacturer's instructions. After 5 h, the fresh medium replaced the medium containing transfection reagents, and cells were further infected with ASFV. The sequences of ZBP1-specific siRNA oligonucleotide are as follows: 5'-CCAGAGGCUUCCAUGAUATT-3'.

2.7 Real-time qPCR for determination of ZBP1 gene expression

Total RNA was extracted from PAMs using the TRIzol reagent and reverse transcribed using the PrimeScript RT kit (TaKaRa). qPCR was performed using the PowerUp SYBR Green Master Mix

on the ABI StepOnePlus system. All data were analyzed using the StepOnePlus software, and the relative mRNA level of ZBP1 was normalized based on the porcine glyceraldehyde 3-phosphate dehydrogenase (GAPDH) mRNA level. Furthermore, the relative mRNA level of ZBP1 was determined based on the comparative cycle threshold ($2^{-\Delta\Delta CT}$) method. The primer sequences are as follows:

- Porcine ZBP1-F: 5'-GAAGGGACTGAACAACTGCA-3'
- Porcine ZBP1-R: 5'-CGTCGGAGGGAGGTAGAA-3'
- Porcine GAPDH-F: 5'-ACATGGCCTCCAAGGAGTAAGA-3'
- Porcine GAPDH-R: 5'-GATCGAGTTGGGGCTGTGACT-3'.

2.8 Real-time qPCR detecting ASFV genome copies

ASFV genomic DNA in infected cells was extracted using QIAamp DNA Mini Kits (Qiagen, Germany). RT-qPCR was performed using the Pro Taq HS premix Probe qPCR kit (Accurate Biology, China) and the QuantStudio5 system (Applied Biosystems, USA). The targeting gene for amplification of the ASFV genome was the conserved B646L gene segment, using the following primers:

- ASFV-P72-F: 5'-GATACCACAAGATCAGCCGT-3'
- ASFV-P72-R: 5'-CTGCTCATGGTATCAATCTTATCGA-3'
- TaqMan probe: 5'-CCACGGGAGGAATACCAACCCAGTG-3'.

The amplification conditions used to detect ASFV genome copies were as follows: preheating at 95°C for 30 s; 40 cycles at 95°C for 5 s; and annealing at 58°C for 30 s; elongation (72°C). The copy numbers of the ASFV genome were calculated using an established standard curve and presented in genome copies per milliliter.

2.9 Viral titration

The ASFV CN/GS/2018 strain was quantified using hemadsorption (HAD) assays with minor modifications. Briefly, PAMs and porcine red blood cells were seeded in 96-well plates. The samples containing ASFV were then added to the plates and titrated in 10-fold serial dilutions. HAD was observed on day 7 post-inoculation, and 50% of HAD doses (HAD50) were calculated according to the Reed–Muench method.

2.10 Co-immunoprecipitation

ASFV-infected PAMs were lysed in NP-40 lysis buffer supplemented with 1 mM phenylmethanesulfonyl fluoride. Cell lysates were incubated on ice for 30 min and briefly sonicated, then high-speed centrifugation (12,000 rpm/min, 10 min) at 4°C. After saving 10% of the total cell lysate

for input, the extracts were divided into two parts for immunoprecipitation with anti-ZBP1 or mouse IgG at 4°C overnight. Subsequently, protein G agarose beads (Roche) were added to the cell lysate and incubated for 3 h at 4°C. Finally, beads were centrifuged (8,000 rpm/min, 30 s) and washed thrice with PBS buffer. The protein-antibody-beads complex was added to the SDS-loading buffer and further detected by immunoblotting.

2.11 Immunoblotting analysis

The proteins with different molecular weights were separated by 8% using SDS-PAGE (80 V, 30 min; 120 V, 60 min) and then transferred to a nitrocellulose membrane (100 V, 90 min). The protein-loaded nitrocellulose membrane was blocked with bovine serum albumin (5%) for 1 h at normal temperature and incubated with the designated antibodies at 4°C overnight. HRP-conjugated anti-mouse/rabbit IgG was incubated to bind the designated antibodies. After developing an electrochemiluminescence solution, the immunoblotting images were captured by the Odyssey infrared imaging system.

2.12 Indirect immunofluorescence assay

Cells were plated on 20 mm glass-bottom cell culture dishes in diameter (NEST) and allowed to adhere for at least 8 h before the next experiments. Following ASFV infection or other treatments, cells were fixed in freshly prepared 4% (w/v) paraformaldehyde, permeabilized in 0.2% (v/v) Triton X-100, blocked with 5% BSA (Sigma), and incubated overnight with primary antibodies at 4°C. Then, dishes were incubated with fluorophore-conjugated secondary antibodies for 2 h at room temperature. Following three additional washes in PBS, the cell nucleus was stained with 4-methyl-6-phenylindole for 10 min and imaged by confocal microscopy on a Leica SP8 instrument. Fluorescence intensity was quantified using Leica LAS X software.

2.13 Cytotoxicity assay

PAMs and BMDMs were cultured in 48-well cell culture plates. The supernatant was discarded after cell adhesion, and the cells were infected with ASFV. After 2 h, the viral fluid was replaced with a fresh 1640 culture medium containing 2% FBS. At the indicated times, the cell supernatant was collected and checked immediately. Cytoplasmic membrane damage was detected by measuring cytoplasmic lactate dehydrogenase (LDH) release using Promega CytoTox 96[®] Non-Radioactive Cytotoxicity Assay kit (J2380) according to the manufacturer's instructions. Luminescence was measured on a Synergy HT Multi-Detection microplate reader (Bio-Tek). Relative LDH release was calculated as the ratio of LDH release of experimental samples to maximum release.

2.14 ELISA assay

PAMs and BMDMs were cultured in 48-well cell culture plates. The supernatant was discarded after cell adhesion, and the cells were infected with ASFV. After 2 h, the viral fluid was replaced with a fresh 1640 culture medium containing 2% FBS. At the indicated times, the cell supernatant was collected and checked immediately. The concentrations of porcine TNF- α (RAB047) in supernatants were measured using the ELISA Kit (Sigma-Aldrich) according to the manufacturer's instructions. The concentrations of porcine IL-1 β (ESIL1B) in culture supernatants were measured using the ELISA Kit (InvitrogenTM) according to the manufacturer's instructions.

2.15 Z-DNA sequences prediction

The Z-forming potential of the genome sequence of ASFV CN/GS/2018 was determined by the ZHUNT3 program (<https://github.com/Ho-Lab-Colostate/zhunt>) using the following command line "zhunt3nt 12 6 24." Data are presented using Microsoft Excel.

2.16 Statistical analysis

All *in vitro* experiments were performed at least three times. Data are presented as the means \pm standard deviations (SDs). The statistical significance between groups was determined using the *t*-test with GraphPad Prism v.8 (San Diego, CA, USA). * $p < 0.05$, ** $p < 0.01$, *** $p < 0.001$, **** $p < 0.0001$ was considered statistically significant. ns: no significant difference.

3 Results

3.1 ASFV infection activated the necroptosis signaling *in vivo*

Pigs were intramuscularly injected with 1 HAD50 of the parent virus ASFV CN/GS/2018 (ASFV-WT) or PBS to explore whether ASFV activates necroptosis signaling. Two pigs infected with ASFV showed clinical symptoms associated with ASF, such as anorexia, stumbling gait, and diarrhea. The ASFV load in the blood continued to increase in ASFV-infected pigs, and tissue testing also showed that ASFV replicated effectively *in vivo* (Figures 1A, B). Western blot results showed that the expression and phosphorylation levels of RIPK3 and MLKL in these tissue samples were the hallmarks of necroptosis. The results showed that the expression and phosphorylation levels of RIPK3 and MLKL were undetectable or faint in healthy pigs' spleen, lung, liver, and kidney. However, the expression and phosphorylation levels of RIPK3 and MLKL were significantly upregulated in ASFV-infected spleen, lung, liver, and kidney (Figure 1C). Therefore, necroptosis signaling was efficiently activated by ASFV in pigs' spleen, lung, liver and kidney.

3.2 ASFV infection efficiently induces macrophage necroptosis *in vitro*

Next, the necroptosis signaling in ASFV-infected primary PAMs and porcine bone marrow-derived macrophages (BMDMs) was analyzed. ASFV replicated efficiently in PAMs and BMDMs, and its proliferation kinetics are shown in Supplementary Figure S1.

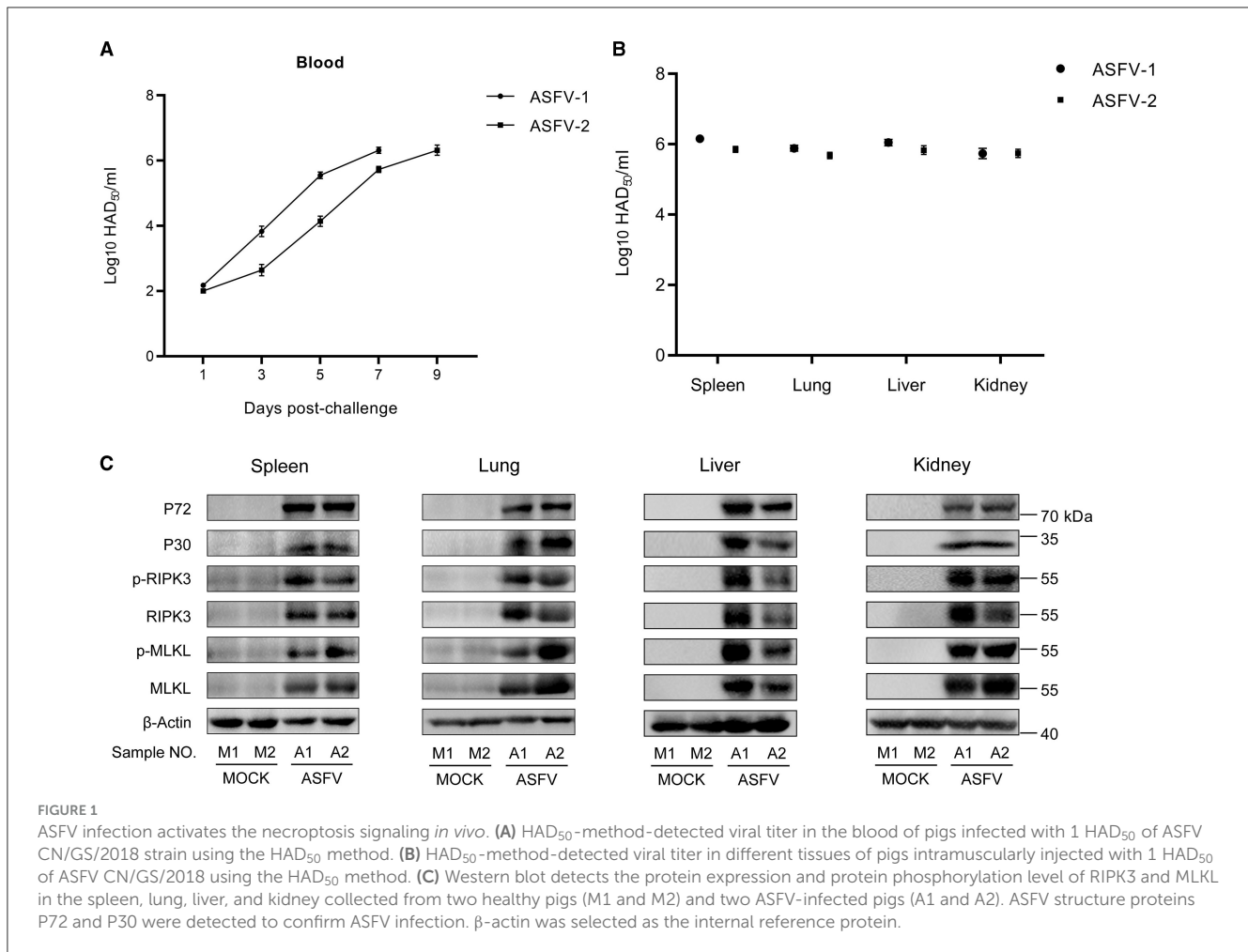
After infecting PAMs and BMDMs with ASFV in dose-dependent or time-dependent ways, the expression and phosphorylation levels of RIPK3 and MLKL were analyzed using western blot, and the cytoplasmic membrane integrity of ASFV-infected macrophages also was determined by cytotoxicity analysis.

The results indicated that the expression of RIPK3 and the phosphorylation levels of RIPK3 and MLKL were significantly elevated in ASFV-infected PAMs and BMDMs in a dose- and time-dependent manner (Figures 2A, C, E, G). This was similar to the data from ASFV-infected porcine tissues. In contrast, MLKL was expressed constructively in PAMs and BMDMs. Furthermore, the release of cytoplasmic lactate dehydrogenase (LDH) in the supernatants of ASFV-infected PAMs and BMDMs was significantly increased in a dose- and time-dependent manner, indicating that the cytoplasmic membrane of host macrophages was damaged during ASFV infection (Figures 2B, D, F, H). Together, these results confirmed that ASFV infection induces macrophage necroptosis *in vitro*.

3.3 ASFV-induced necroptosis signaling is independent of the TNF- α -RIPK1 pathway in macrophages

ASFV infection induced the high-level secretion of porcine TNF- α (Carrasco et al., 2002; Salguero et al., 2002; Zheng et al., 2022). RIPK1-dependent necroptosis can be enhanced by overexpressing ASFV A179L (Shi et al., 2021). We sought to determine whether ASFV-induced macrophage necroptosis depends on the TNF- α -RIPK1 pathway. PAMs and BMDMs were treated with recombinant interferon- β (IFN- β) to induce the expression of RIPK3, then cotreated with TSZ (T: TNF α ; S: SM-164; Z: Z-VAD-FMK) as the positive necroptosis control dependent on the TNF- α -RIPK1 pathway. Necrostatin-1 (Nec-1, an inhibitor of kinase activity of RIPK1) was added to inhibit TNF- α -RIPK1 signaling in macrophages. Inhibitors GSK'872 (an inhibitor of the kinase activity of RIPK3) or GW806742X (an inhibitor of MLKL) were used to suppress necroptosis signaling activated via any pathway.

As shown in Figures 3A, B, the treatment of GSK'872 or GW806742X resulted in the obvious inhibition of MLKL phosphorylation and the release of LDH in ASFV-infected or TSZ-treated PAMs. While Nec-1 treatment significantly inhibited the phosphorylation of RIPK3 and MLKL and the release of LDH in TSZ-treated PAMs, a similar effect of Nec-1 was not observed in ASFV-infected PAMs. Similar to data from ASFV-infected PAMs, Nec-1 also failed to alleviate the phosphorylation of RIPK3 and MLKL and the release of



LDH in ASFV-infected BMDMs (Figures 3C, D). Therefore, the TNF α -RIPK1 pathway is dispensable for ASFV-induced macrophage necroptosis.

3.4 ASFV-induced necroptosis signaling is independent of the TLR-TRIF pathway in macrophages

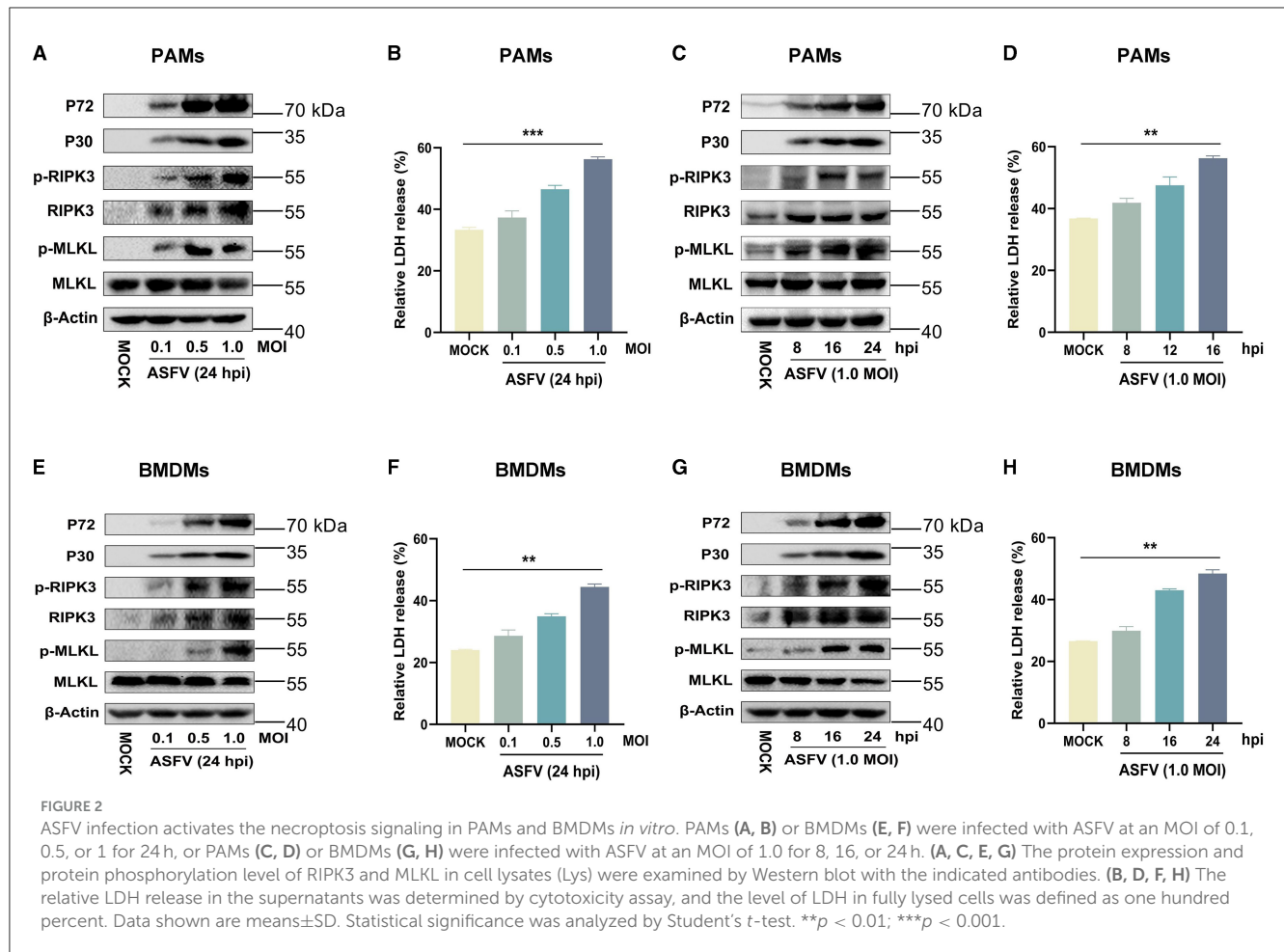
TLR3 (an innate immune receptor sensing dsRNA) and TLR4 (an innate immune receptor sensing LPS) are important to the expression of IL-1 β in ASFV-infected PAMs (Li J. et al., 2021). We further investigated whether ASFV-induced macrophage necroptosis is dependent on the TLR3/4-TRIF pathway. PAMs and BMDMs were cotreated with IFN- β , LPS, and Z-VAD-FMK as the positive necroptosis control dependent on the TLR4-TRIF pathway. Pepinh-TRIF (TFA, a peptide blocking TLR-TRIF interaction) was added to inhibit TLR-TRIF signaling in macrophages.

The results showed that TFA treatment significantly inhibited the phosphorylation of RIPK3 and MLKL and

the release of LDH in LPS-induced PAMs and BMDMs necroptosis. However, the TFA still did not suppress the necroptosis signaling in PAMs and BMDMs induced by ASFV infection (Figure 4). Therefore, these results indicated that ASFV-induced macrophage necroptosis is independent of the TLR-TRIF pathway.

3.5 ZBP1 necrosome is essential for ASFV-induced macrophage necroptosis

In addition to RIPK1 and TRIF, ZBP1 (an IFN-stimulated gene) is the third RHIM-containing host protein that recruits RIPK3 to activate necroptosis signaling. Consequently, the effect of ZBP1 on ASFV-induced macrophage necroptosis was explored further. Our past research on transcriptomics and proteomics of ASFV-infected host macrophages revealed that ZBP1 upregulates with interferon expression in macrophages during ASFV infection (Figure 5A) (Yang et al., 2021, 2023). The upregulation of ZBP1 was further confirmed by quantitative reverse transcriptase PCR (qRT-PCR) and western blot analysis on ASFV-infected PAMs (Figures 5B, C). Further, an indirect immunofluorescence assay



was performed to illuminate the spatial relationship between ZBP1 and ASFV infection. The results showed high-level ZBP1 was detected in ASFV-infected macrophages but not in uninfected cells (Figure 5D).

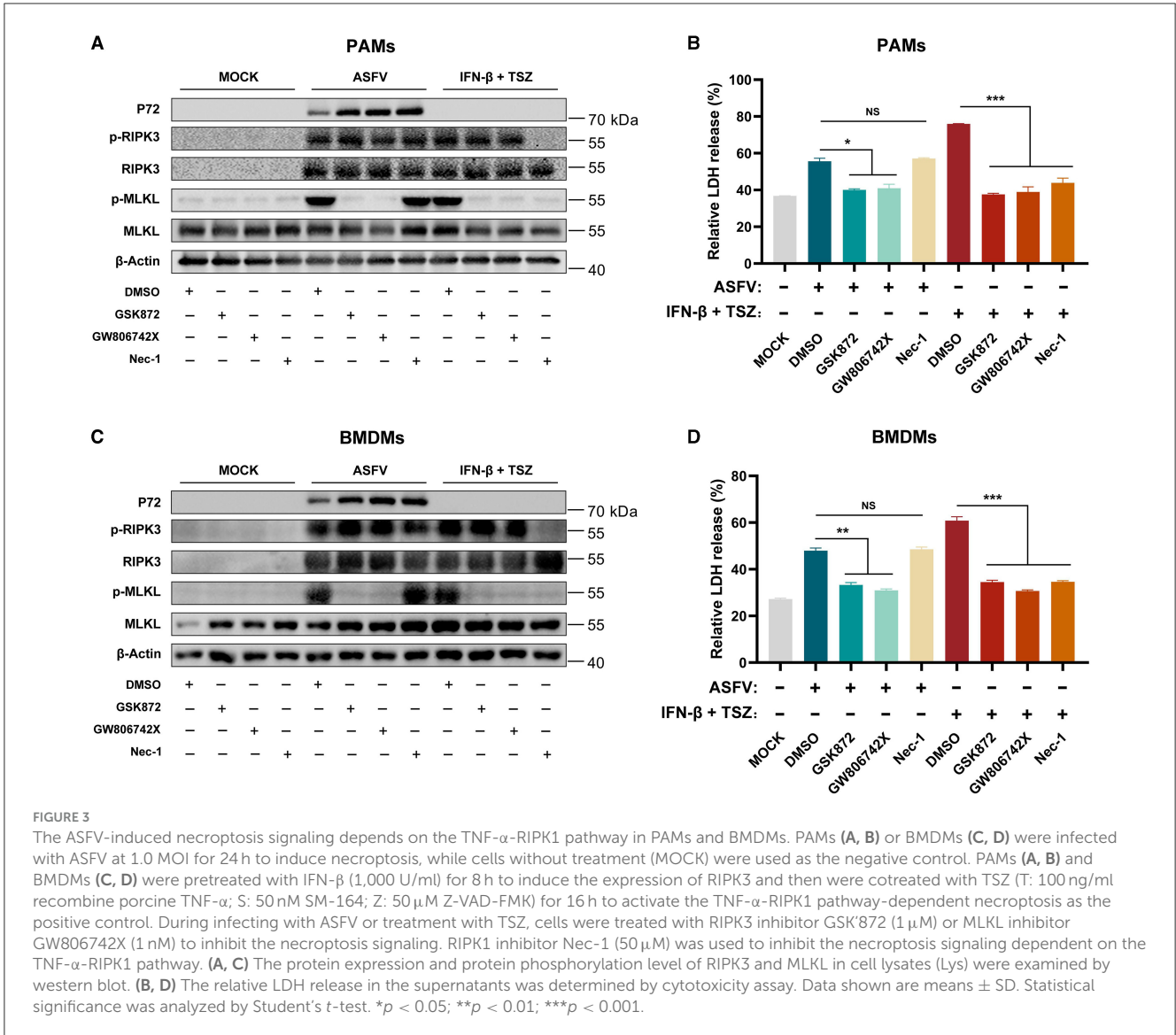
To further explore the connection between ZBP1 and macrophage necroptosis during ASFV infection, endogenous co-immunoprecipitation (Co-IP) assays were conducted with ASFV-infected PAMs using anti-ZBP1 antibody. PAMs without any treatment (MOCK) were used as the negative control, and IFN- β -stimulated PAMs were used as infection-free controls expressing ZBP1 and RIPK3. The results of the western blot showed that ZBP1 and RIPK3 were both highly expressed in IFN- β -stimulated and ASFV-infected PAMs. Interestingly, while ZBP1 did not interact with RIPK3 and MLKL in MOCK or IFN- β -stimulated PAMs, significant interaction between ZBP1, RIPK3, and MLKL was observed in PAMs with ASFV infection (Figure 5E). These results demonstrated that ZBP1 necrosome composed of ZBP1, RIPK3, and MLKL was successfully assembled during ASFV infection.

To further confirm the importance of ZBP1 on ASFV-induced macrophage necroptosis, the upregulated expression of ZBP1 in PAMs was knocked down by transfecting siRNA targeting ZBP1 mRNA. Then, the ASFV-induced necroptosis signaling was analyzed. Western blot results indicated that the phosphorylation

of RIPK3 and MLKL was inhibited when ZBP1 upregulation disappeared in PAMs infected with ASFV (Figure 5F). Moreover, ASFV-induced release of LDH was also dramatically alleviated in ZBP1-knocking down PAMs (Figure 5G). These findings demonstrated that ASFV infection upregulates the ZBP1 expression to consist of necrosome and induce macrophage necroptosis.

3.6 Z-DNA form and are recognized by ZBP1 in ASFV-infected PAMs

Sensing the virus-derived Z-nucleic acid (Z-NA) is critical for ZBP1 to activate necroptosis during virus infection (Balachandran and Mocarski, 2021). Considering that the ZBP1 necrosome is only assembled with ASFV infection (Figure 5D), we hypothesized that ASFV infection generates the viral-derived Z-NA to activate ZBP1. Therefore, the propensity to form Z-DNA sequences in the ASFV genome was first analyzed to test this hypothesis. Continuous (GC)_n in double-stranded nucleic acids is likely to form the Z-conformations, and the Z-forming potential of ASFV can be scored computationally by the Z-HUNT3 algorithm (Ho, 2009). The results of the Z-HUNT3 algorithm showed that the proportion of G and C in the ASFV CN/GS/2018 genome was ~40%, but



the ASFV genome was predicted to contain multiple potential Z-DNA sequences (Figures 6A, B). Past studies have confirmed that anti-Z-NA antibody (Z22) can recognize virus-derived Z-NA as the activated ligand recognized by the ZBP1 sensor. The same antibody was used to verify whether ASFV infection generates Z-NA. As shown in Figure 6C, the specific Z-NA signals were clearly observed in ASFV-infected PAMs with labeled anti-P30 and anti-Z-NA antibodies. Because Z-NA antibodies only recognize the Z conformation of double-stranded NA but do not distinguish whether it is Z-DNA or Z-RNA, ASFV-infected PAMs were further treated with RNase A or DNase I. Indirect immunofluorescence assay (IFA) results showed that the treatment with RNase A had no significant effect on the accumulation of Z-NA signal (Figures 6D, F). In contrast, DNase I treatment strongly reduced the Z-NA signals (Figures 6E, F), suggesting that the detected Z-NA within ASFV-infected PAMs was Z-DNA. Interestingly, we found that the Z-DNA signals were distributed

in both the cytoplasm and nucleus of PAMs infected with ASFV (Figures 6C, D).

To investigate the relationship between ZBP1 and Z-DNA during ASFV infection, the subcellular localization of ZBP1 and Z-DNA in PAMs infected with ASFV was further analyzed by IFA. IFA results showed a distinct co-localization between ZBP1 and Z-DNA in the cytoplasm and the nucleus of ASFV-infected PAMs (Figures 6G, H). We also examined the subcellular location of ZBP1 following ASFV infection by separating the nucleus and cytoplasm components. The western blot results showed that ZBP1 was preferentially upregulated in the nucleus at 8 hours post-infection (hpi) and subsequently appeared in the cytoplasm at 12 hpi. The MLKL was also phosphorylated initially in the nucleus and then in the cytoplasm of ASFV-infected PAMs (Figure 6I), suggesting that the ZBP1-mediated necroptosis signaling was activated in the cytoplasm and nucleus of ASFV-infected cells.

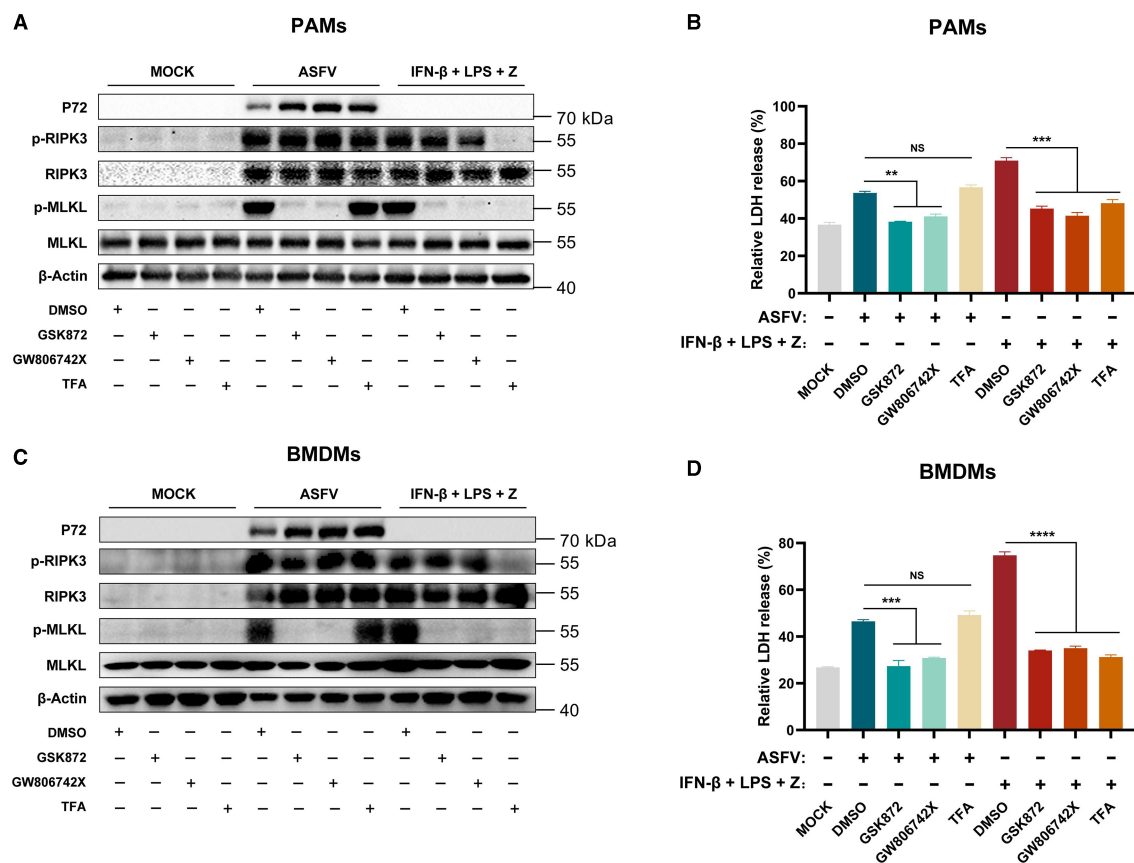


FIGURE 4

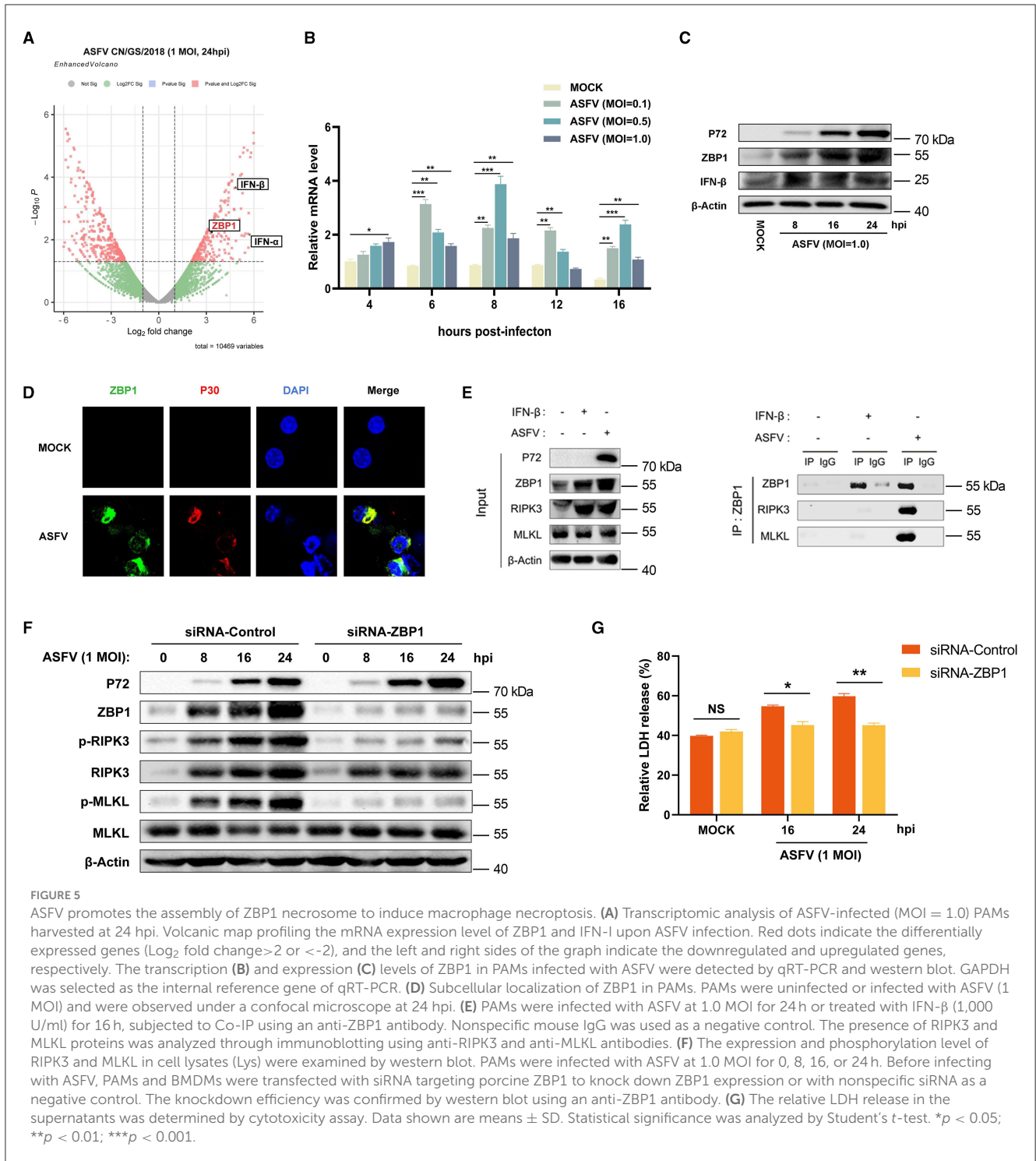
The ASFV-induced necroptosis signaling depends on the TLR-TRIF pathway in PAMs and BMDMs. PAMs (A, B) or BMDMs (C, D) were infected with ASFV at 1.0 MOI for 24 h to induce necroptosis, while cells without treatment (MOCK) were used as the negative control. PAMs (A, B) and BMDMs (C, D) were pretreated with IFN-β (1,000 U/ml) for 8 h to induce the expression of RIPK3 and then were treated with LPS (100 ng/ml) plus Z-VAD-FMK (50 μM) for 24 h to activate the TLR4-TRIF pathway-dependent necroptosis as the positive control. During infecting with ASFV or treatment with LPS plus Z-VAD-FMK, cells were treated with GSK872 (1 μM) or GW806742X (1 nM) to inhibit the necroptosis signaling. TFA (the interaction inhibitor between TLR and TRIF) (40 μM) inhibited the necroptosis signaling dependent on the TLR-TRIF pathway. (A, C) The protein expression and protein phosphorylation level of RIPK3 and MLKL in cell lysates (Lys) were examined by western blot. (B, D) The relative LDH release in the supernatants was determined by cytotoxicity assay. Data shown are means ± SD. Statistical significance was analyzed by Student's *t*-test. ***p* < 0.01; ****p* < 0.001; *****p* < 0.0001.

The $Z\alpha$ domain of ZBP1 is important for sensing accumulated Z-NA and its nuclear migration (Zhang et al., 2020; Hao et al., 2022). By reconstituting the Myc-tagged ZBP1 mutant plasmid lacking the $Z\alpha 2$ domain (Myc-ZBP1 $\Delta Z\alpha 2$) that was based on the Myc-tagged porcine wild-type ZBP1 plasmid (Myc-ZBP1^{WT}) (Supplementary Figure S2), the role of the $Z\alpha 2$ domain on the ZBP1 nucleus localization after ASFV infection was further investigated. Given that overexpressed plasmids are difficult to transfect into primary macrophages, Myc-ZBP1^{WT} and Myc-ZBP1 $\Delta Z\alpha 2$ plasmids were transfected into MA-104 cells (a passage cell line that can infect ASFV) and then infected with ASFV to observe their subcellular localization (Rai et al., 2020). The results showed that Myc-ZBP1^{WT} and Myc-ZBP1 $\Delta Z\alpha 2$ both localized in the cytoplasm of MA-104 cells uninfected with ASFV, and the p-MLKL signal was not detected. After getting infected with ASFV, partial Myc-ZBP1^{WT} transferred into the nucleus, while the p-MLKL signal was upregulated and colocalized with ZBP1 in the cytoplasm and nucleus of ASFV-infected MA-104 cells. However, compared to Myc-ZBP1^{WT}, Myc-ZBP1 $\Delta Z\alpha 2$ was detained in the cytoplasm of the ASFV-infected MA-104 cells,

which was similar to the subcellular distribution of Myc-ZBP1 $\Delta Z\alpha 2$ expressed in uninfected MA-104 cells (Figure 6). Transfected with ZBP1 $\Delta Z\alpha 2$ defective in nuclear localization, nuclear p-MLKL still existed, possibly due to endogenous ZBP1 mediated by MA104. Consequently, the $Z\alpha 2$ domain of ZBP1 plays an important role in response to ASFV-induced nucleus localization of ZBP1.

3.7 ZBP1-mediated macrophage necroptosis facilitates the extracellular release of proinflammatory cytokines induced by ASFV infection

Necroptosis causes cell plasma membrane damage, further resulting in the extracellular release of cytoplasmic proinflammatory cytokines and DAMPs (Kaczmarek et al., 2013). The concentration of proinflammatory cytokines, including porcine TNF-α and IL-1β, in supernatants from ASFV-infected macrophages was measured using ELISA kits. After infection



with ASFV, the concentrations of porcine TNF-α and IL-1β were significantly elevated in supernatants of PAMs and BMDMs in a time-dependent manner (Figures 7A–D).

Furthermore, the effect of ZBP1-mediated necroptosis signaling on ASFV-induced release of TNF-α and IL-1β was investigated. After inhibiting the macrophage necroptosis using inhibitors or siRNA-ZBP1, TNF-α and IL-1β were severely dampened in supernatants of PAMs and BMDMs infected with ASFV (Figures 7E–H). Together, these results demonstrated that ZBP1-mediated necroptosis is the main cause

of the extracellular release of proinflammatory cytokines in ASFV-infected macrophages.

3.8 ZBP1-mediated necroptosis inhibits ASFV replication in macrophages

Necroptosis signaling induces severe inflammation during viral infection but has different effects on viral replication.

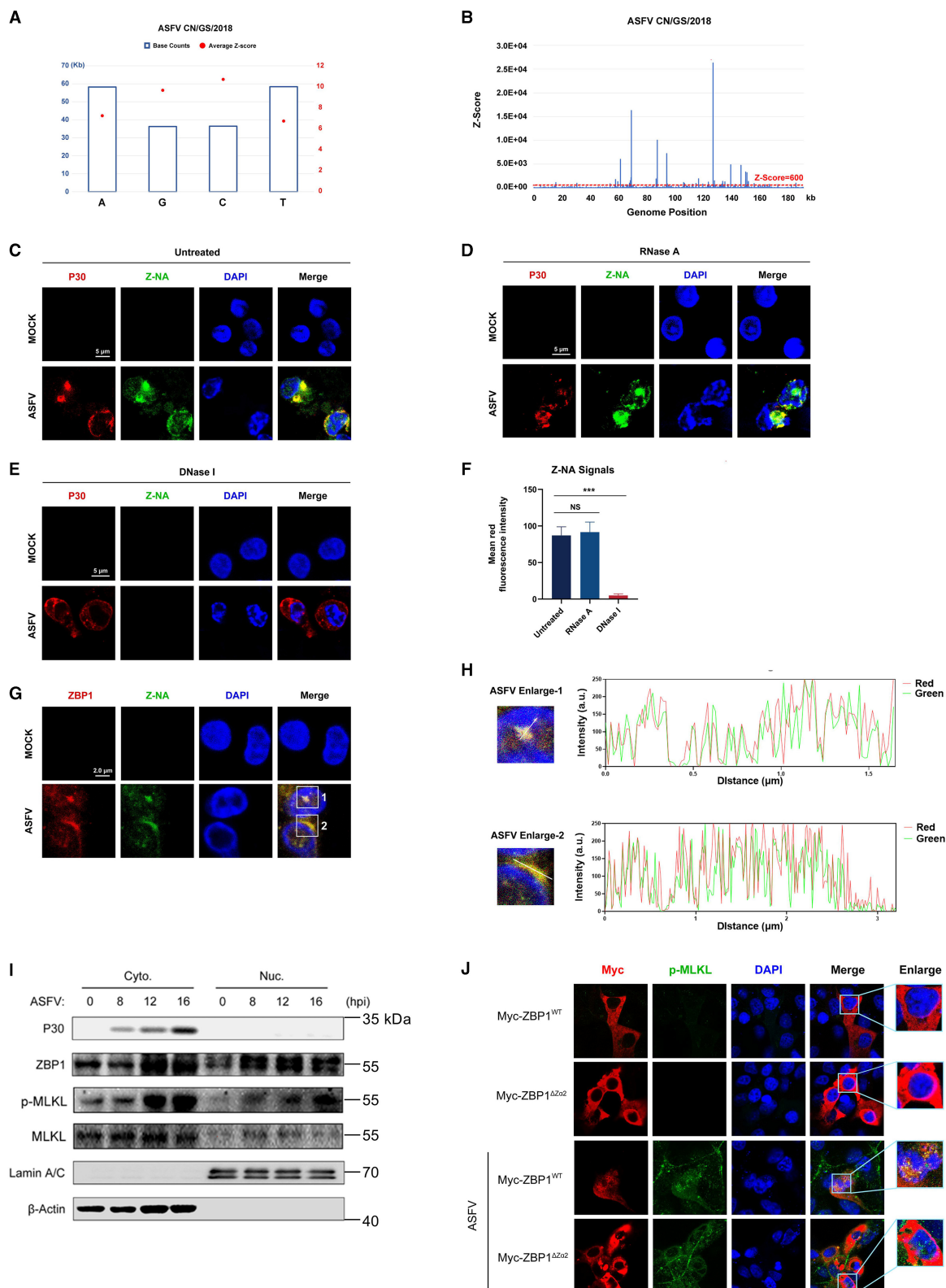


FIGURE 6 Accumulation of Z-DNA in ASFV-infected cells. **(A)** The counts and average Z-score of adenine (A), thymine (T), guanine (G), and cytidine (C) in the ASFV CN/GS/2018 genome. **(B)** The potential Z-DNA sequence in the ASFV genome was analyzed using the Z-HUNT 3 program, which scores the propensity of sequences to flip to the left-handed helical Z-conformation. The red dotted line indicates a Z-score of 600. A Z-score >600 indicates that the sequence tends to form the Z-conformation under physiological conditions. **(C–E)** ASFV CN/GS/2018 (MOI = 1.0) infected or uninfected (Mock) PAMs were fixed and permeabilized at 16 hpi and then either untreated **(C)** or treated with RNase A (1 mg/ml) **(D)** or DNase I (5 U/ml) **(E)**. Cells were co-stained with antibodies against Z-NA (green) and ASFV structure protein P30 (red). Nuclei were stained by DAPI (blue). **(F)** Quantifying the *(Continued)*

FIGURE 6 (Continued)

mean fluorescence intensity (MFI) of Z-NA staining in ASFV-infected cells in C-E. Scale bar, 5 μ m. (G) ASFV CN/GS/2018 (MOI = 1.0) infected PAMs were co-stained with ZBP1 and Z-NA antibodies. (H) Quantitative analysis of the co-localization between ZBP1 and Z-DNA was performed with ImageJ. (I) Immunoblot analysis of ZBP1, p-MLKL, and MLKL in nuclear and cytoplasmic fractions from ASFV-infected (1 MOI) PAMs at the indicated times. Immunoblotting for β -actin and Lamin A/C was used to confirm the purity of cytoplasmic and nuclear fractions. (J) MA-104 cells were transfected with Myc-ZBP1^{WT} or ZBP1 Δ Z α 2 and then infected with ASFV (MOI = 1.0) to analyze the ZBP1 localization at 16 hpi. ASFV infection was indicated by co-staining for p-MLKL in the same cells. Scale bars represent 5 μ m (C, D, E, G, J). Data shown are means \pm SD. Statistical significance was analyzed by Student's *t*-test. ****p* < 0.001.

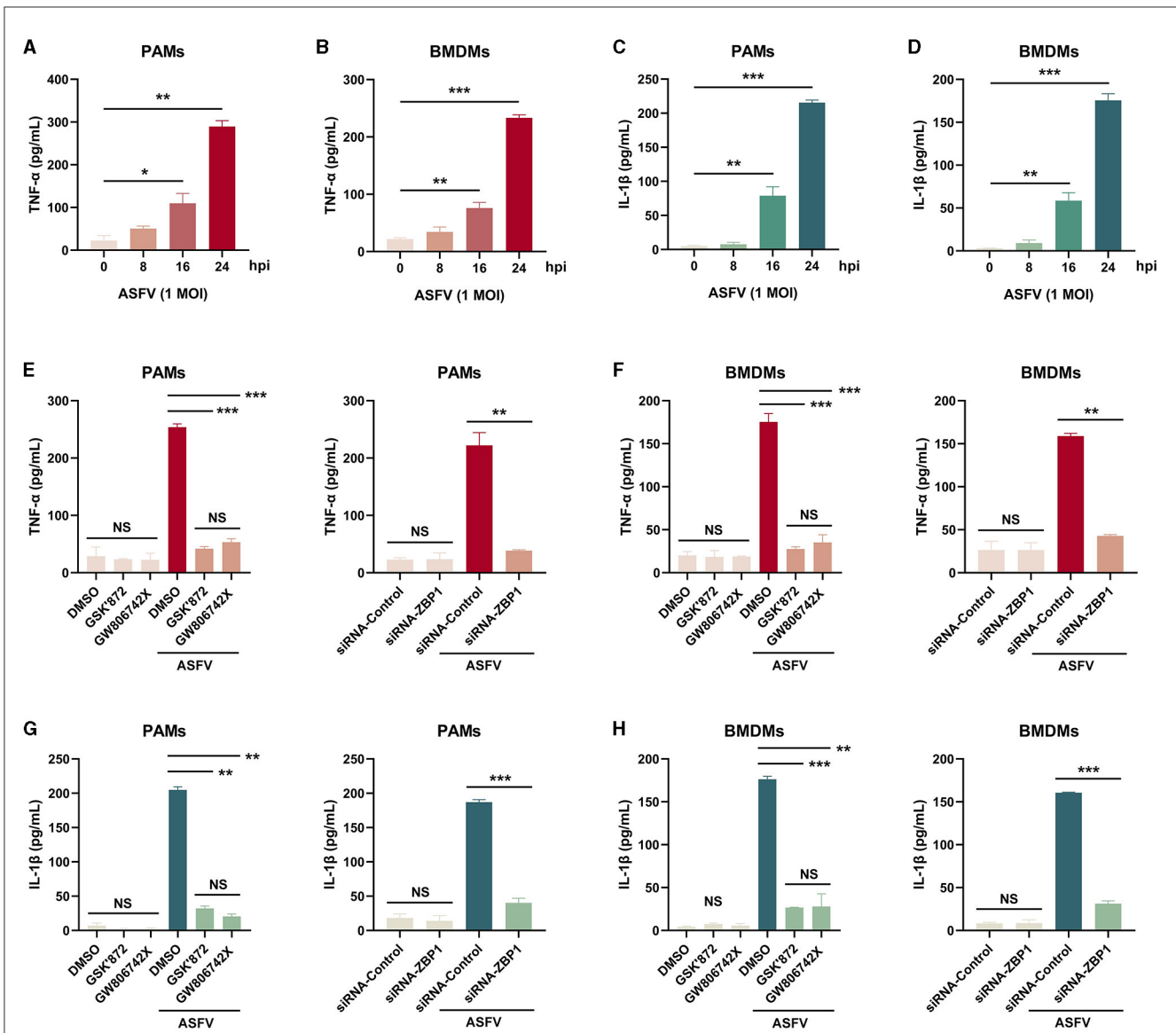


FIGURE 7

The extracellular release of TNF- α and IL-1 β was restrained in ASFV-infected macrophages by inhibiting the ZBP1-mediated necroptosis. The TNF- α (A, B, E, F) and mature IL-1 β (C, D, G, H) levels in the supernatants were determined by ELISA. PAMs (A, C, E, G) and BMDMs (B, D, F, H) were infected with ASFV at 1.0 MOI for indicated times. (E, F, G, H) PAMs and BMDMs were treated with GSK872 (1 μ M) or GW806742X (1 nM) to inhibit necroptosis or were added to DMSO as a control. (E, F, G, H) PAMs and BMDMs were transfected with siRNA-ZBP1 or siRNA-control before infecting with ASFV. Data shown are means \pm SD. Statistical significance was analyzed by Student's *t*-test. **p* < 0.05; ***p* < 0.01; ****p* < 0.001.

Western blot results showed that the expression of ASFV P72 was upregulated in necroptosis-inhibited macrophages by treating inhibitors or transfecting siRNA-ZBP1. We finally examined the role of ZBP1-mediated macrophage necroptosis on ASFV replication. After treatment with inhibitors or siRNA, the ASFV genome copies and viral titer in PAMs and BMDMs infected

with ASFV were determined by qRT-PCR and HAD₅₀ assay. The results indicated that the ASFV genome copies and viral titer were slightly increased in necroptosis-inhibited PAMs and BMDMs, demonstrating that the ZBP1-mediated necroptosis signaling inhibits ASFV replication in macrophages *in vitro* (Figure 8).

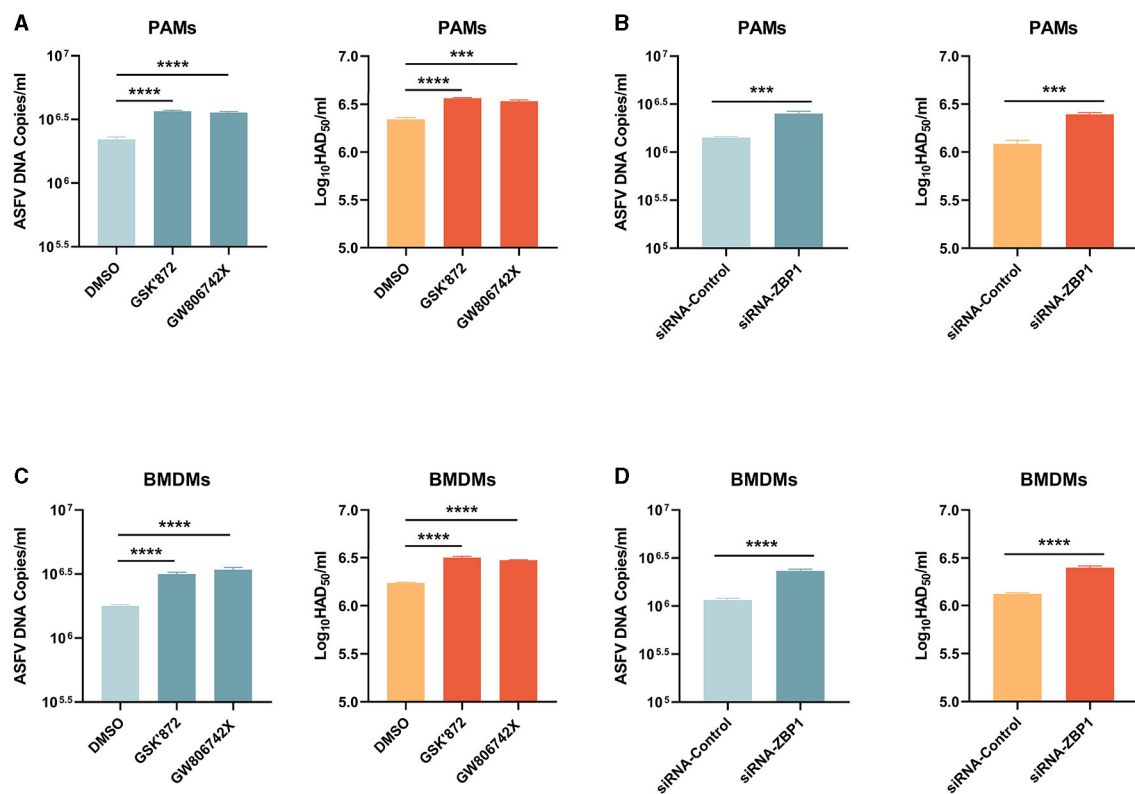


FIGURE 8

ASFV replication was boosted in PAMs and BMDMs, in which necroptosis was inhibited. PAMs (A, B) and BMDMs (C, D) were infected with ASFV at 1.0 MOI for 24 h. PAMs (A) and BMDMs (C) were treated with GSK'872 (1 μ M) or GW806742X (1 nM) to inhibit necroptosis during infection. PAMs (B) and BMDMs (D) were transfected with siRNA-ZBP1 before infecting with ASFV. ASFV genome copies and viral titer were determined by qRT-PCR and HAD50. Data shown are means \pm SD. Statistical significance was analyzed by Student's *t*-test. ****p* < 0.001; *****p* < 0.0001.

4 Discussion

Macrophages, highly plastic cells in the host immune system, are important for activating innate and adaptive immunity against microbes while causing various pathologies during infectious diseases (Murray and Wynn, 2011). The interactions between ASFV and porcine macrophages play a critical role in ASFV-induced pathological lesions, whereas little is known about the ASFV-macrophage interaction and molecular mechanism (Salguero, 2020). We showed that ASFV infection activates the necroptosis signaling in the porcine spleen, lung, liver, and kidney (Figure 1), and porcine macrophage necroptosis was induced by ASFV infection *in vitro* (Figure 2). Hemorrhagic or hyperaemic splenomegaly is the most obvious lesion in ASFV-infected pigs (Carrasco et al., 1997). The histopathology of the ASFV-infected spleen mainly renders a hyperaemic red pulp, even filled with red blood cells (Salguero, 2020). The macrophage population of porcine splenic red pulp has predominantly anchored a mesh of fibers in the splenic cords, surrounded by smooth muscle cells (Carrasco et al., 1995). The macrophage death in the red pulp causes damage to intercellular junctions between the smooth muscle cells and further bares the basal lamina, followed by the activation of the coagulation cascade, platelet aggregation, and fibrin deposition, finally accumulating red blood cells within the splenic cords

(Gomez-Villamandos et al., 2013; Salguero, 2020). Consequently, the ASFV-induced macrophage necroptosis may explain why ASFV infection results in hemorrhagic or hyperaemic splenomegaly.

Mechanically, TNF- α expression was induced by ASFV (Salguero et al., 2002). Overexpressing ASFV A179L enhanced the TNF- α -induced and RIPK1-dependent necroptosis (Shi et al., 2021), and TLR3 and TLR4 were activated to induce the IL-1 β expression in ASFV-infected PAMs (Li J. et al., 2021). Nevertheless, our findings indicated that the TNF- α -RIPK1 and TLR-TRIF signaling pathways are not the primary pathways responsible for ASFV-induced macrophage necroptosis (Figures 3, 4). RIPK1 is an important adapter protein for signaling transduction, including necroptosis, apoptosis, pyroptosis, and MAPK signaling (Wang Q. et al., 2021). Many viral proteins target RIPK1 to suppress the RIPK1-mediated signaling. For instance, Murine cytomegalovirus (MCMV) encoded M45 and herpes simplex virus 1 (HSV-1) encoded ICP6 both inhibit the necroptosis signaling by disrupting the RIPK1-RIPK3 interaction (Sridharan et al., 2017; Ali et al., 2019; Muscolino et al., 2020). Similarly, the Epstein-Barr virus (EBV) encoded LMP1 interacts with and ubiquitinates RIPK1 to suppress necroptosis (Liu et al., 2018). Therefore, certain proteins encoded by ASFV can inhibit TNF- α -induced necroptosis by targeting RIPK1. Additionally, ASFV I329L has been identified as an inhibitor of TLR3 signaling by targeting TRIF (de Oliveira

et al., 2011), which might also contribute to suppressing TLR-TRIF pathway-dependent necroptosis.

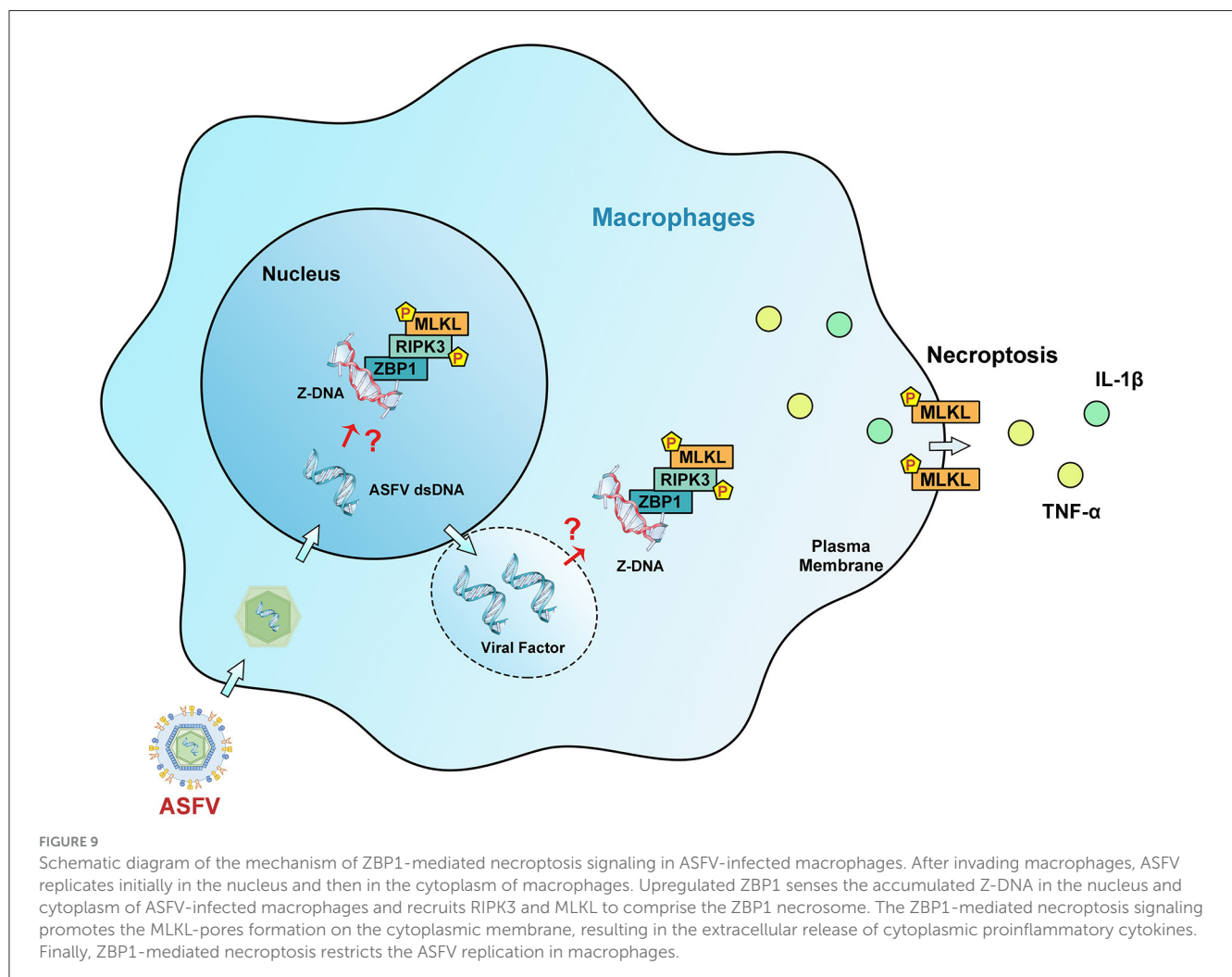
ZBP1 was originally identified as an innate immune sensor that activates interferon (IFN) responses and NF- κ B signaling (Takaoka et al., 2007). Recently, ZBP1 has been reported as the master protein inducing PANoptosis (pyroptosis, apoptosis, and necroptosis) (Hao et al., 2022). Our past and present results confirmed that ZBP1 expression was significantly upregulated in host macrophages infected with ASFV (Figures 5A–D) (Yang et al., 2021, 2023). The upregulated ZBP1 interacts with RIPK3 and MLKL to consist of the ZBP1-RIPK3-MLKL necrosome and activate macrophage necroptosis during ASFV infection (Figures 5E–G).

Virus infection-induced ZBP1 activation needs ZBP1 to sense the virus-derived Z-RNA (Koehler et al., 2017; Zhang et al., 2020; Li et al., 2023). However, Z-DNA sequences were predicted to be present in the ASFV genome using the Z-HUNT3 program (Figure 6B). Additional experiments confirmed the accumulation of Z-DNA signals in both the nucleus and cytoplasm of ASFV-infected cells. In contrast, Z-RNA signals did not accumulate (Figures 6C–F).

ASFV has always been considered a cytoplasmic DNA virus; it replicates in the viral factory around the nucleus. However, studies

have confirmed that early replication of ASFV occurs in the nucleus (Ortin and Vinuela, 1977; Simoes et al., 2015). Thus, we suspect that the Z-DNA recognized by ZBP1 is derived from the genomic dsDNA of ASFV, which is accumulated in both the nucleus and cytoplasm of macrophages during ASFV replication. Nevertheless, more experiments are needed to confirm this hypothesis.

The subcellular distribution of ZBP1-mediated necroptosis signaling mainly depends on the ZBP1 recognition for its Z-NA ligands. Influenza A virus (IAV) replication generates Z-RNA in the nucleus so that ZBP1 initiates necroptosis activation in the nucleus and results in nuclear envelope disruption leakage of DNA into the cytosol (Zhang et al., 2020). However, ZBP1 recognized viral Z-RNA and activated necroptosis in the cytoplasm of vaccinia virus (VACV) or SARS-CoV-2 infected cells (Koehler et al., 2017; Li et al., 2023). Past studies have confirmed that early replication of ASFV occurs in the nucleus and subsequently replicates in the perinuclear viral factory (Ortin and Vinuela, 1977; Simoes et al., 2015). Our finding demonstrated the co-localization between ZBP1 and Z-DNA in the nucleus and the cytoplasm of ASFV-infected cells (Figures 6G, H), activated the nucleus and cytoplasmic necroptosis signaling (Figure 6I). However, in ASFV-infected cells, we did not observe the clear leakage of nuclear chromatin and DNA into



the cytosol, similar to the IAV-infected cells. Consequently, the effect of nucleus necroptosis signaling in ASFV-infected cells is currently unknown.

The virus-infected monocyte-macrophages extensively express and secrete proinflammatory cytokines, including TNF- α and IL, described as cytokines storm (Carrasco et al., 2002; Zheng et al., 2022). Our findings indicated that ASFV infection induces the massive secretion of TNF- α and IL-1 β in macrophages, but IFN- γ and IL-18 do not change (Figure 7). Either pyroptosis or necroptosis contributes to the extracellular release of cytoplasmic proinflammatory cytokines by damaging the cytoplasm membrane. We found that the extracellular levels of TNF- α and IL-1 β were almost completely blocked and dampened when ASFV-induced macrophage necroptosis was inhibited (Figure 7). During IAV and SARS-CoV-2 infection, infected cells released proinflammatory cytokines that were significantly alleviated only when pyroptosis and necroptosis were both inhibited. This difference may be attributed to the GSDMD inactivation caused by ASFV pS273R, causing ASFV-induced proinflammatory cytokines to only be released from macrophages via MLKL-pores (Zhao et al., 2022).

ZBP1-mediated necroptosis effectively restricts the ASFV infection in macrophages (Figure 8). However, the ZBP1-dependent PANoptosis-mediated cytokines storm usually results in severe organ dysfunction and clinical symptoms. The inflammatory cell infiltration and alveolar septa expansion caused by SARS-CoV-2 infection were meaningfully alleviated after knocking down RIPK3 (Karki et al., 2022; Li et al., 2023). Necroptotic cells act as impactful immunogenic to recruit and activate neutrophils. Further, bronchioalveolar necroptosis is also the reason for IAV-induced acute respiratory distress syndrome (ARDS) (Momota et al., 2020). Hemorrhagic lesions caused by ASFV are primarily due to the release of cytokines from infected macrophages rather than direct damage to endothelial cells (Gomez-Villamandos et al., 2013). We also confirmed that ASFV activated necroptosis signaling in porcine lungs and PAMs, which may be related to respiratory distress and severe hemorrhages in the septa and the alveolar spaces for ASFV-infected pigs (Carrasco et al., 1996; Salguero, 2020). Massive destruction of the lymphoid organs and tissues, including the spleen and lymph nodes, are the most important features in ASFV pathology. A large proportion of B and T lymphocytes undergo cell death in acute ASFV infection (Salguero et al., 2004; Fernández de Marco et al., 2007). In immune organs, signaling interaction between lymphocytes and macrophages is key to triggering the adaptive immune response. However, during ASFV infection, ZBP1-mediated necroptotic macrophages release TNF- α and IL-1 β that cause lymphocyte apoptosis (Gómez del Moral et al., 1999). Therefore, ASFV-induced macrophage necroptosis may be a key pathway by which ASFV disrupts the porcine adaptive immune system.

In conclusion, this work demonstrates that ASFV can induce macrophage necroptosis by promoting ZBP1 necrosome activation. It also uncovers the mechanism by which Z-DNA in ASFV-infected cells is recognized by ZBP1 to induce necrosome assembly. ZBP1-mediated necroptosis signaling causes the release of proinflammatory cytokines and inhibits ASFV replication

in macrophages (Figure 9). Regrettably, whether ZBP1-mediated macrophage necroptosis is beneficial or harmful for host immunity against ASFV infection still requires further animal experiments to elucidate. Together, these findings extend our knowledge about the interaction between ASFV and macrophage necroptosis and shed light on the pathogenesis of ASFV.

Data availability statement

The original contributions presented in the study are included in the article/Supplementary material, further inquiries can be directed to the corresponding author.

Ethics statement

The animal study was approved by the experimental procedures were approved by the Ethic Committee of Lanzhou Veterinary Research Institute, Chinese Academy of Agricultural Sciences. The approval number was License No. SYXK [GAN] 2014-003. The study was conducted in accordance with the local legislation and institutional requirements.

Author contributions

DZhan: Conceptualization, Investigation, Writing – original draft. YH: Conceptualization, Validation, Writing – original draft. XY: Investigation, Writing – review & editing. XS: Investigation, Writing – review & editing. DZhao: Investigation, Validation, Writing – review & editing. LC: Validation, Writing – review & editing. HL: Validation, Writing – review & editing. ZZ: Writing – review & editing. HZ: Funding acquisition, Writing – review & editing.

Funding

The author(s) declare financial support was received for the research, authorship, and/or publication of this article. This work was supported by grants from the National Key R&D Program of China (2021YFD1801300), the Major Science and Technology project of Gansu Province, China (22ZD6NA001, 22ZD6NA012), National Swine Technology Innovation Center of China (NCTIP-XD/C03, CARS-35), and the Institute of Animal Health, Guangdong Academy of Agricultural Sciences of China (2022SDZG02).

Acknowledgments

The authors would like to thank all the editors and reviewers for their valuable comments and suggestions that helped improve the quality of this manuscript. The authors would also like to thank the other members of the HZ lab for their constructive comments.

Conflict of interest

The authors declare that the research was conducted in the absence of any commercial or financial relationships that could be construed as a potential conflict of interest.

Publisher's note

All claims expressed in this article are solely those of the authors and do not necessarily represent those of their affiliated

organizations, or those of the publisher, the editors and the reviewers. Any product that may be evaluated in this article, or claim that may be made by its manufacturer, is not guaranteed or endorsed by the publisher.

Supplementary material

The Supplementary Material for this article can be found online at: <https://www.frontiersin.org/articles/10.3389/fmicb.2024.1419615/full#supplementary-material>

References

- Ali, M., Roback, L., and Mocarski, E. S. (2019). Herpes simplex virus 1 ICP6 impedes TNF receptor 1-induced necrosome assembly during compartmentalization to detergent-resistant membrane vesicles. *J. Biol. Chem.* 294, 991–1004. doi: 10.1074/jbc.RA118.004651
- Alonso, C., Borca, M., Dixon, L., Revilla, Y., Rodriguez, F., Escibano, J. M., et al. (2018). ICTV virus taxonomy profile: Asfarviridae. *J. Gen. Virol.* 99, 613–614. doi: 10.1099/jgv.0.001049
- Balachandran, S., and Mocarski, E. S. (2021). Viral Z-RNA triggers ZBP1-dependent cell death. *Curr. Opin. Virol.* 51, 134–140. doi: 10.1016/j.coviro.2021.10.004
- Carrasco, L., Bautista, M. J., Gómez-Villamandos, J. C., Martín de las Mulas, J., Chacón, M. L. F., Wilkinson, P. J., et al. (1997). Development of microscopic lesions in splenic cords of pigs infected with African swine fever virus. *Vet. Res.* 28, 93–99.
- Carrasco, L., Bautista, M. J., Martín de las Mulas, J., Gómez-Villamandos, J. C., Espinosa de los Monteros, A., and Sierra, M. A. (1995). Description of a new population of fixed macrophages in the splenic cords of pigs. *J. Anat.* 187(Pt 2), 395–402.
- Carrasco, L., deLara, F. C., GomezVillamandos, J. C., and Bautista, M. J. (1996). The pathogenic role of pulmonary intravascular macrophages in acute African swine fever. *Res. Vet. Sci.* 61, 193–198. doi: 10.1016/S0034-5288(96)90062-4
- Carrasco, L., Nunez, A., Salguero, F. J., San Segundo, F. D., Sanchez-Cordon, P., Gomez-Villamandos, J. C., et al. (2002). African swine fever: expression of interleukin-1 alpha and tumour necrosis factor-alpha by pulmonary intravascular macrophages. *J. Comp. Pathol.* 126, 194–201. doi: 10.1053/jcpa.2001.0543
- de Oliveira, V. L., Almeida, S. C., Soares, H. R., Crespo, A., Marshall-Clarke, S., and Parkhouse, R. M. (2011). A novel TLR3 inhibitor encoded by African swine fever virus (ASFV). *Arch. Virol.* 156, 597–609. doi: 10.1007/s00705-010-0894-7
- Fernández de Marco, M., Salguero, F. J., Bautista, M. J., Núñez, A., Sánchez-Cordón, P. J., and Gómez-Villamandos, J. C. (2007). An immunohistochemical study of the tonsils in pigs with acute African swine fever virus infection. *Res. Vet. Sci.* 83, 198–203. doi: 10.1016/j.rvsc.2006.11.011
- Galindo, I., Hernaez, B., Diaz-Gil, G., Escibano, J. M., and Alonso, C. (2008). A179L, a viral Bcl-2 homologue, targets the core Bcl-2 apoptotic machinery and its upstream BH3 activators with selective binding restrictions for Bid and Noxa. *Virology* 375, 561–572. doi: 10.1016/j.virol.2008.01.050
- Galindo, I., Hernaez, B., Munoz-Moreno, R., Cuesta-Geijo, M. A., Dalmau-Mena, I., Alonso, C., et al. (2012). The ATF6 branch of unfolded protein response and apoptosis are activated to promote African swine fever virus infection. *Cell Death Dis.* 3:e341. doi: 10.1038/cddis.2012.81
- Gallardo, M. C., Reoyo, A. T., Fernandez-Pinero, J., Iglesias, I., Munoz, M. J., Arias, M. L., et al. (2015). African swine fever: a global view of the current challenge. *Porcine Health Manag.* 1:21. doi: 10.1186/s40813-015-0013-y
- Gómez del Moral, M., Ortuño, E., Fernández-Zapatero, P., Alonso, F., Alonso, C., Ezquerro, A., et al. (1999). African swine fever virus infection induces tumor necrosis factor alpha production: implications in pathogenesis. *J. Virol.* 73, 2173–2180. doi: 10.1128/JVI.73.3.2173-2180.1999
- Gomez-Villamandos, J. C., Bautista, M. J., Sanchez-Cordon, P. J., and Carrasco, L. (2013). Pathology of African swine fever: the role of monocyte-macrophage. *Virus Res.* 173, 140–149. doi: 10.1016/j.virusres.2013.01.017
- Grootjans, S., Vanden Berghe, T., and Vandenabeele, P. (2017). Initiation and execution mechanisms of necroptosis: an overview. *Cell Death Differ.* 24, 1184–1195. doi: 10.1038/cdd.2017.65
- Hao, Y., Yang, B., Yang, J., Shi, X., Yang, X., Zhang, D., et al. (2022). ZBP1: a powerful innate immune sensor and double-edged sword in host immunity. *Int. J. Mol. Sci.* 23:10224. doi: 10.3390/ijms231810224
- Ho, P. S. (2009). Thermogenomics: thermodynamic-based approaches to genomic analyses of DNA structure. *Methods* 47, 159–167. doi: 10.1016/j.jmeth.2008.09.007
- Kaczmarek, A., Vandenabeele, P., and Krysko, D. V. (2013). Necroptosis: the release of damage-associated molecular patterns and its physiological relevance. *Immunity* 38, 209–223. doi: 10.1016/j.immuni.2013.02.003
- Karki, R., Lee, S., Mall, R., Pandian, N., Wang, Y., Sharma, B. R., et al. (2022). ZBP1-dependent inflammatory cell death, PANoptosis, and cytokine storm disrupt IFN therapeutic efficacy during coronavirus infection. *Sci Immunol* 7:eab06294. doi: 10.1126/sciimmunol.abo6294
- Koehler, H., Cotsmire, S., Langland, J., Kibler, K. V., Kalman, D., Upton, J. W., et al. (2017). Inhibition of DAI-dependent necroptosis by the Z-DNA binding domain of the vaccinia virus innate immune evasion protein, E3. *Proc. Natl. Acad. Sci. USA.* 114, 11506–11511. doi: 10.1073/pnas.1700999114
- Li, J., Song, J., Kang, L., Huang, L., Zhou, S., Hu, L., et al. (2021). pMGF505-7R determines pathogenicity of African swine fever virus infection by inhibiting IL-1beta and type I IFN production. *PLoS Pathog.* 17:e1009733. doi: 10.1371/journal.ppat.1009733
- Li, S., Zhang, Y., Guan, Z., Ye, M., Li, H., You, M., et al. (2023). SARS-CoV-2 Z-RNA activates the ZBP1-RIPK3 pathway to promote virus-induced inflammatory responses. *Cell Res.* 33, 201–214. doi: 10.1038/s41422-022-00775-y
- Li, T., Zhao, G., Zhang, T., Zhang, Z., Chen, X., Song, J., et al. (2021). African swine fever virus pE199L induces mitochondrial-dependent apoptosis. *Viruses* 13:2240. doi: 10.3390/v13112240
- Liu, X., Li, Y., Peng, S., Yu, X., Li, W., Shi, F., et al. (2018). Epstein-Barr virus encoded latent membrane protein 1 suppresses necroptosis through targeting RIPK1/3 ubiquitination. *Cell Death Dis.* 9:53. doi: 10.1038/s41419-017-0081-9
- Momota, M., Lelliott, P., Kubo, A., Kusakabe, T., Kobiyama, K., Kuroda, E., et al. (2020). ZBP1 governs the inflammasome-independent IL-1 α and neutrophil inflammation that play a dual role in anti-influenza virus immunity. *Int. Immunol.* 32, 203–212. doi: 10.1093/intimm/dxz070
- Murphy, J. M. (2020). The killer pseudokinase mixed lineage kinase domain-like protein (MLKL). *Cold Spring Harb. Perspect. Biol.* 12:a036376. doi: 10.1101/cshperspect.a036376
- Murray, P. J., and Wynn, T. A. (2011). Protective and pathogenic functions of macrophage subsets. *Nat. Rev. Immunol.* 11, 723–737. doi: 10.1038/nri3073
- Muscolino, E., Schmitz, R., Loroch, S., Caragliano, E., Schneider, C., Rizzato, M., et al. (2020). Herpesviruses induce aggregation and selective autophagy of host signalling proteins NEMO and RIPK1 as an immune-evasion mechanism. *Nat. Microbiol.* 5, 331–342. doi: 10.1038/s41564-019-0624-1
- Nogal, M. L., Gonzalez de Buitrago, G., Rodriguez, C., Cubelos, B., Carrascosa, A. L., Salas, M. L., et al. (2001). African swine fever virus IAP homologue inhibits caspase activation and promotes cell survival in mammalian cells. *J. Virol.* 75, 2535–2543. doi: 10.1128/JVI.75.6.2535-2543.2001
- Ortin, J., and Vinuela, E. (1977). Requirement of cell nucleus for African swine fever virus replication in vero cells. *J. Virol.* 21, 902–905. doi: 10.1128/jvi.21.3.902-905.1977
- Rai, A., Pruitt, S., Ramirez-Medina, E., Vuono, E. A., Silva, E., Velazquez-Salinas, L., et al. (2020). Identification of a continuously stable and commercially available cell line for the identification of infectious african swine fever virus in clinical samples. *Viruses* 12:820. doi: 10.3390/v12080820
- Salguero, F. J. (2020). Comparative pathology and pathogenesis of african swine fever infection in swine. *Front. Vet. Sci.* 7:282. doi: 10.3389/fvets.2020.00282
- Salguero, F. J., Ruiz-Villamor, E., Bautista, M. J., Sanchez-Cordon, P. J., Carrasco, L., Gomez-Villamandos, J. C., et al. (2002). Changes in macrophages in spleen and

- lymph nodes during acute African swine fever: expression of cytokines. *Vet. Immunol. Immunopathol.* 90, 11–22. doi: 10.1016/S0165-2427(02)00225-8
- Salguero, F. J., Sánchez-Cordón, P. J., Sierra, M. A., Jover, A., Núñez, A., Gómez-Villamandos, J. C., et al. (2004). Apoptosis of thymocytes in experimental African swine fever virus infection. *Histol. Histopathol.* 19, 77–84. doi: 10.14670/HH-19.77
- Sanchez-Cordon, P. J., Montoya, M., Reis, A. L., and Dixon, L. K. (2018). African swine fever: a re-emerging viral disease threatening the global pig industry. *Vet. J.* 233, 41–48. doi: 10.1016/j.tvjl.2017.12.025
- Shi, J., Liu, W., Zhang, M., Sun, J., and Xu, X. (2021). The A179L gene of African swine fever virus suppresses virus-induced apoptosis but enhances necroptosis. *Viruses* 13:2490. doi: 10.3390/v13122490
- Simoes, M., Martins, C., and Ferreira, F. (2015). Early intranuclear replication of African swine fever virus genome modifies the landscape of the host cell nucleus. *Virus Res.* 210, 1–7. doi: 10.1016/j.virusres.2015.07.006
- Sridharan, H., Ragan, K. B., Guo, H., Gilley, R. P., Landsteiner, V. J., Kaiser, W. J., et al. (2017). Murine cytomegalovirus IE3-dependent transcription is required for DAI/ZBP1-mediated necroptosis. *EMBO Rep.* 18, 1429–1441. doi: 10.15252/embr.201743947
- Takaoka, A., Wang, Z., Choi, M. K., Yanai, H., Negishi, H., Ban, T., et al. (2007). DAI (DLM-1/ZBP1) is a cytosolic DNA sensor and an activator of innate immune response. *Nature* 448, 501–505. doi: 10.1038/nature06013
- Urbano, A. C., and Ferreira, F. (2022). African swine fever control and prevention: an update on vaccine development. *Emerg. Microbes Infect.* 11, 2021–2033. doi: 10.1080/22221751.2022.2108342
- Verdonck, S., Nemegeer, J., Vandenabeele, P., and Maelfait, J. (2022). Viral manipulation of host cell necroptosis and pyroptosis. *Trends Microbiol.* 30, 593–605. doi: 10.1016/j.tim.2021.11.011
- Wang, Q., Fan, D., Xia, Y., Ye, Q., Xi, X., Zhang, X. G., et al. (2021). The latest information on the RIPK1 post-translational modifications and functions. *Biomed. Pharmacother.* 142:112082. doi: 10.1016/j.biopha.2021.112082
- Wang, Y., Kang, W., Yang, W., Zhang, J., Li, D., Zheng, H., et al. (2021). Structure of African swine fever virus and associated molecular mechanisms underlying infection and immunosuppression: a review. *Front. Immunol.* 12:715582. doi: 10.3389/fimmu.2021.715582
- Xia, X., Lei, L., Wang, S., Hu, J., and Zhang, G. (2020). Necroptosis and its role in infectious diseases. *Apoptosis* 25, 169–178. doi: 10.1007/s10495-019-01589-x
- Yang, B., Hao, Y., Yang, J., Zhang, D., Shi, X., Yang, X., et al. (2023). PI3K-Akt pathway-independent PIK3AP1 identified as a replication inhibitor of the African swine fever virus based on iTRAQ proteomic analysis. *Virus Res.* 327:199052. doi: 10.1016/j.virusres.2023.199052
- Yang, B., Shen, C., Zhang, D., Zhang, T., Shi, X., Yang, J., et al. (2021). Correction to: Mechanism of interaction between virus and host is inferred from the changes of gene expression in macrophages infected with African swine fever virus CN/GS/2018 strain. *Virology* 18, 186. doi: 10.1186/s12985-021-01654-5
- Yu, P., Zhang, X., Liu, N., Tang, L., Peng, C., Chen, X., et al. (2021). Pyroptosis: mechanisms and diseases. *Signal Transduct. Target. Ther.* 6:128. doi: 10.1038/s41392-021-00507-5
- Zhang, T., Yin, C., Boyd, D. F., Quarato, G., Ingram, J. P., Shubina, M., et al. (2020). Influenza virus Z-RNAs induce ZBP1-mediated necroptosis. *Cell* 180, 1115–1129.e1113. doi: 10.1016/j.cell.2020.02.050
- Zhao, G., Li, T., Liu, X., Zhang, T., Zhang, Z., Kang, L., et al. (2022). African swine fever virus cysteine protease pS273R inhibits pyroptosis by noncanonically cleaving gasdermin D. *J. Biol. Chem.* 298:101480. doi: 10.1016/j.jbc.2021.101480
- Zheng, Y. X., Li, S., Li, S. H., Yu, S. X., Wang, Q. H., Zhang, K. H., et al. (2022). Transcriptome profiling in swine macrophages infected with African swine fever virus at single-cell resolution. *Proc. Natl. Acad. Sci. USA.* 119:e2201288119. doi: 10.1073/pnas.2201288119
- Zhou, P., Dai, J., Zhang, K., Wang, T., Li, L. F., Luo, Y., et al. (2022). The H240R protein of African Swine fever virus inhibits interleukin 1beta production by inhibiting NEMO expression and NLRP3 oligomerization. *J. Virol.* 96:e0095422. doi: 10.1128/jvi.00954-22
- Zhou, X., Li, N., Luo, Y., Liu, Y., Miao, F., Chen, T., et al. (2018). Emergence of African swine fever in China, 2018. *Transbound. Emerg. Dis.* 65, 1482–1484. doi: 10.1111/tbed.12989